Design of an underground railway station beneath a historic building in Rome and class A predictions of the induced effects

Progettazione di una stazione ferroviaria sotterranea sotto un edificio storico a Roma e previsioni di classe A degli effetti indotti

Salvatore MILIZIANO[a]
Simone CAPONI[b]
David CARLACCINI[b]
Armando DE LILLIS[a*]

[a] Sapienza University of Rome, Rome, Italy
[b] Geotechnical Design Group, Rome, Italy
* corresponding author: armando.delillis@uniroma1.it

Abstract
The railway station Flaminio, currently located at street level, will be relocated underground to connect the railway with the existing line A metro station. This paper describes the technical and technological solutions adopted in the design to minimize tunnelling-induced effects on the surface and, in particular, on an old masonry building, whose foundations are very close to the roof of the new three-tunnel station. To reduce the risks, pre-confinement works and soil improvements were designed; furthermore, a very stiff pre-support system consisting of 36 horizontal steel pipes filled with concrete, located just above the tunnels and installed using a special Micro Tunnel Boring Machine, was devised. The paper also presents the numerical models developed both in 2D and 3D to study the soil-structure interaction and the class A predictions in terms of expected settlements and potential damages induced.

Sommario
La stazione ferroviaria Flaminio, attualmente situata in superficie, sarà presto sostituita da una nuova stazione sotterranea, con l'obiettivo di collegare la linea ferroviaria esistente con la linea A della metropolitana di Roma. L'articolo descrive le soluzioni tecniche e tecnologiche adottate nel progetto per minimizzare i cedimenti indotti in superficie e, soprattutto, gli effetti su un edificio di pregio in muratura, le cui fondazioni raggiungono profondità prossime al tetto della nuova stazione. Al fine di ridurre i rischi, il progetto prevede importanti interventi di pre-confinamento del fronte di scavo. Inoltre, è previsto un sistema di pre-sostegno, situato appena al di sopra delle gallerie di stazione, costituito da 36 tubolari in acciaio riempiti di calcestruzzo e installato mediante una speciale Micro Tunnel Boring Machine, appositamente progettata. L'articolo descrive anche i modelli numerici sviluppati in 2D e 3D per studiare l'interazione terreno-struttura e le previsioni numeriche di classe A in termini di cedimenti e potenziali danni indotti.

Keywords: tunnelling, soil-structure interaction, settlements, micro TBM, 3D numerical modelling.

1. Introduction

When tunnelling in urban areas, the interference with surrounding structures and infrastructures is a crucial concern. In European cities in particular, the historical and architectural importance of the interacting buildings is often an additional reason to introduce in the underground works protective measures aimed at minimizing the induced effects and the risk of damaging pre-existing structures.
Since the risks increase as the tunnel cover decreases, over the past few decades several ingenious technical solutions were developed to allow safe - both in terms of tunnel stability and induced damages - tunnelling under very low covers. Among these it is certainly worth mentioning the mechanical pre-cutting, that enables building concrete shells that serve as roof support prior to each excavation stage. These pre-vaults can also be pre-loaded through mechanical jacks before the excavation realizing the so-called active vaults, as in the case of the metro station of Baldo degli Ubaldi, in Rome [1]. Another effective technique is the cellular arch, first adopted in the construction of the Venezia station of the Milan railway link, which allows to realize the entire ground support structures and the tunnel lining before the excavation [2].

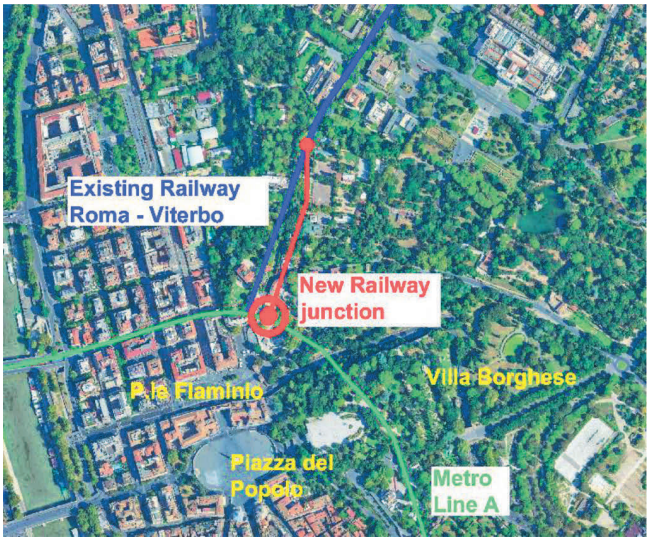

Figure 1. Location of the new Flaminio station.

A further innovative technique was implemented for the construction of the tunnel approaching the AV railways Bologna Central Station, where horizontal pipes filled by concrete were installed close to the tunnel excavation profile before tunnelling, as protective measure.

Settlements due to tunnelling can be assessed, at least at a preliminary stage, employing simple approaches as the Gaussian curves proposed by Peck [3] and then improved by Moh et al. [4], while the damages induced on pre-existing building can be evaluated following the approach originally proposed by Burland and Wroth [5] and then extended by Boscardin and Cording [6] and Burland [7]. As the design stages progress, more advanced approaches must be adopted. The soil-tunnel-building interaction can be simulated using 2D numerical models, as shown by several Authors, among which Miliziano et al. [8], Tamagnini et al. [9], Altamura et al. [10] and Möller and Vermeer [11]. Being two-dimensional, all these methods need to drastically simplify the real phenomena and thus assume various simplifications regarding the three-dimensionality of the excavation process and existing structures. More rigorously, tunnel excavations can be modelled adopting fully three-dimensional approaches. These allow to simulate explicitly the main characteristics of the excavation process, both in conventional [12, 13, 14] and mechanized tunnelling [15, 16 17, 18], and are also more suited to properly account for the hydro-mechanical coupling in cases where the excavation and consolidation times are comparable, as reported by Callari and Casini [19, 20]. Furthermore, 3D numerical models allow to investigate accurately the interaction between soil, tunnel and existing building either using equivalent solids [21, 22, 23, 24] or complete structural models [25, 26, 27, 28].

The great advantage of a fully 3D numerical approach is that by explicitly simulating the main features of the excavation (including complex geometries and work sequences) that influence the induced effects, the settlements trough and the subsidence volume are analysis results and not initial assumptions as is the case with simpler approaches. This makes 3D modelling an excellent tool to quantitatively support the design choices, especially those related to the induced settlements and the associated risks. It is also worth noting that three-dimensional models are becoming progressively more manageable, both in terms of actual runtime, due to faster algorithms and more powerful computers, and set-up time, due to more user-friendly commercial codes.

This paper focuses on the effects induced by the excavation of a three-tunnel station on a historic masonry building in the centre of Rome. As the tunnels underpass the building's foundation with a very low (locally absent) cover, significant protective measures were adopted. Specifically, a pre-support system composed of 36 steel pipes filled with concrete was installed just above the tunnels using a Micro Tunnel Boring Machine (MTBM) and heavy ground improvement works were designed to strengthen and stiffen the excavation front and the soil nucleus behind it.

In the following, after a brief description of the entire project and the characterization of the building and soils involved, the design solution will be thoroughly described illustrating both the main

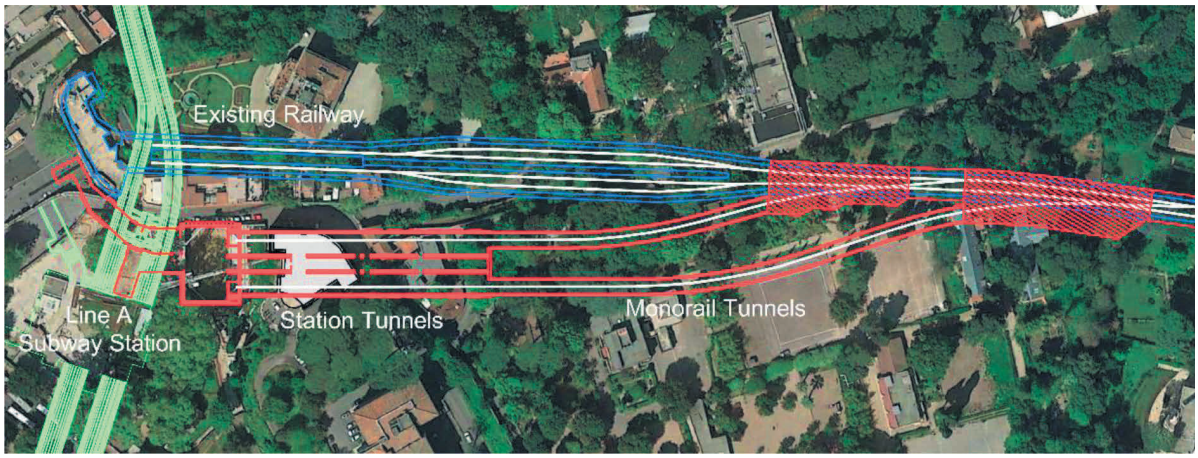

Figure 2. Plan view of the new works and the existing network of connections in Piazzale Flaminio.

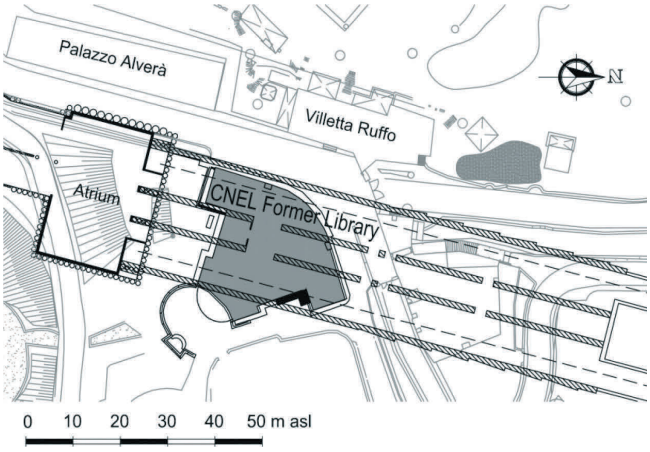

Figure 3. Plan view of the area of the new station.

technical aspects and the class A numerical predictions, also comparing the results of 2D and 3D numerical analyses.

2. The project

The Rome-Civita Castellana-Viterbo regional railway is a major access line to the Italian capital and it serves an important role for work and school commuters. The transportation system will be enhanced through the construction of a new station in Rome, located in the very centre of Rome, near Piazza del Popolo, inside the wonderful Villa Borghese (Fig. 1). The project is financed by the regional authority Regione Lazio and the local transportation authority ATAC was appointed for the management of the construction and the financial relations with the Contractor (FER. RO.VIT Scarl).
The new station's atrium will allow direct access to the station's tunnels from Piazzale Flaminio and underground connection with the existing Flaminio line A metro station. The works also involve the excavation of the station tunnels, and of monorail tunnels connecting the new station with the existing railway (Fig. 2).
The excavation of the atrium and the station tunnels will take place in a very sensitive urban environment. In fact, the tunnels underpass the historic building of the CNEL (National Council for the Economy and Work) former library and the atrium is located closely to the existing railway station and other important buildings (Palazzo Alverà and Villetta Ruffo), as shown in Figure 3. Moreover, the new atrium is adjacent to the existing metro station and overpasses both its station and line tunnels. Last but not least, the excavation will occur in an area well known for its archaeological richness.
The station is composed of three tunnels that will be realized adopting the conventional tunnelling excavation method. The station tunnels will be around 100 m long and near the entrance will underpass the CNEL former library with a very limited, locally even absent, cover. The lateral tunnels will host the rails and platforms; the central one will have a pedestrian path in the upper part and an emergency evacuation exit in the lower part (Fig. 4). To minimize the effects induced on the building, 36 steel tubes grouted to the surrounding soil and filled with concrete, to be installed using a Micro Tunnel Boring Machine (MTBM) before excavating the tunnels, were designed. At the tunnel entrance, the pipes are structurally connected with a robust three-arched portal founded on large piles.
The entrance portal, the atrium and the other access facilities will be realized with excavation supported by pile-walls and internally reinforced with temporary steel struts. The line tunnels will be excavated using the conventional method too, up to the connection with the existing railway.
In this paper, the design of the station tunnels, especially focusing on the under-passing of the CNEL former library, is treated.

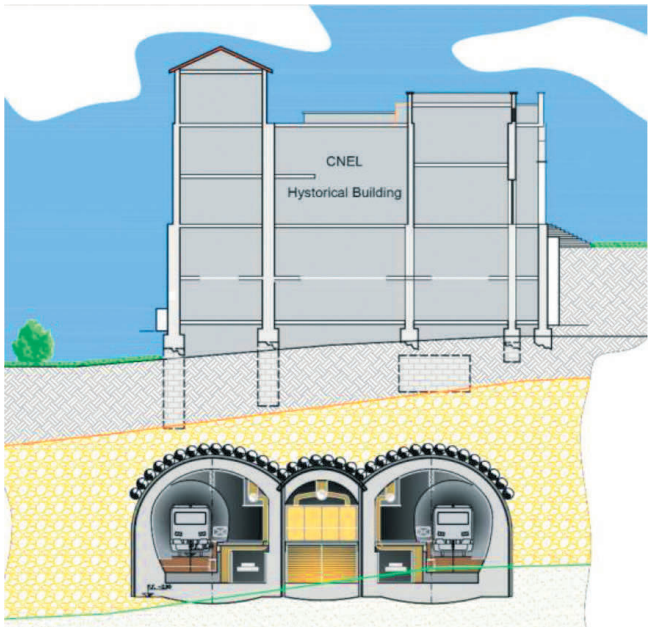

Figure 4. Cross section of the tunnels and the former library of the CNEL.

3. The building and the soils

The geological map of the area, an extract of which is reported in Figure 5, shows the main geological unit found in the area: **qa**) alluvial Pleistocenic deposits with grain size ranging from clays to gravels; **sl3**) stratified tuff, mainly not cemented; **fp**) marsh-fluvial formation made of cemented silt and sand with local volcanic inclusions; **Apl**) deep stratum of stiff and overconsolidated pliocenic silty clays found at the base.
The area interested by the excavation of the station tunnels was studied through several investigation campaigns over the years, both geotechnical and structural. The resulting soil stratigraphy, starting from the top, is the following:
– coarse-grained man-made ground (**R**);
– pleistocenic silty sands, locally cemented, whose thickness varies from few meters near Piazzale Flaminio to about 30 m going north (**S**);

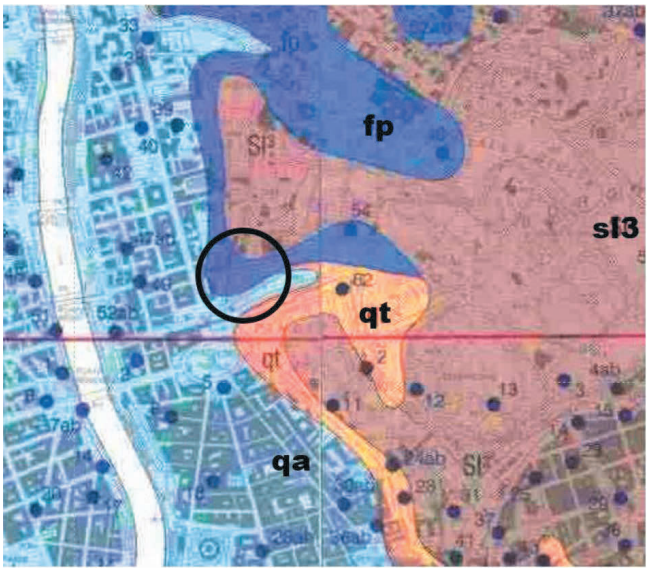

Figure 5. Geological map (modified after Ventriglia [29]).

– sandy gravel with fines, around 5 m thick (**G**);
– the deepest layer, starting from roughly 12 m asl (above sea level), is made of the above-mentioned pliocenic low plasticity silty clays, characterized by good consistency (**Apl**).

The geotechnical characterization of the three upper coarse-grained layers was mainly based on the interpretation of standard penetration test using the correlations proposed by Schmertmann [30] and Denver [31], while the **Apl**'s properties were determined based on laboratory test, pressuremeter test [32, 33] and also taking into account the considerable amount of data available in the technical literature.

Even though more sophisticated approaches can be adopted [34, 35], at the design stage the soil mechanical behaviour was described using a simple elastic perfectly plastic model with Mohr-Coulomb strength criterion and adopting operative stiffness values associated with medium-large strain levels. This is a classic approach aimed at overestimating the induced effects and thus at designing on the side of safety. The adopted characteristic - as defined by the Italian design code

Table 1. Main physical and mechanical characteristic soil parameters.

Soil	γ (kN/m^3)	K_0 (-)	OCR (-)	ν (-)	c' (kPa)	ϕ' (°)	E' (MPa)
R	18.5	0.44	2.0	0.2	5	34	10
S	19.0	0.43	1.2	0.2	70	35	80
G	21.0	0.32	1.2	0.2	0.5	43	70
Apl	20.0	0.82	2.5	0.2	30	28	100

NTC [36] - soil parameters are listed in Table 1, where γ is the unit weight, K_0 the at-rest earth pressure coefficient, *OCR* the overconsolidation ratio, υ the Poisson coefficient, *c'* the effective cohesion, ϕ' the effective friction angle and *E'* the effective Young's modulus. K_0 was calculated according to Mayne and Kulhawy's equation [37]. The soils mainly involved in the tunnels excavation have quite good mechanical characteristics. The large deformations Young's modulus varies in the range 70-100 MPa. **S** and **Apl** are characterized by a high effective cohesion equal to 70 and 30 kPa, respectively. The average effective cohesion of the cemented sand was obtained back-analysing the collapse of an existing cavern close to the work site. The strength of **G** is mainly frictional with a quite high friction angle (43°).

The piezometric regime was determined installing standpipe Casagrande piezometers. The pore-pressures approximately follow a hydrostatic distribution governed by a piezometric surface located at 17 m asl, just above the bottom of the excavation. The water table elevation gently reduces moving toward the existing metro A station, where a well system equipped with pumps actively maintain the water table below the underground station.

The station tunnels will be excavated almost entirely in the sandy stratum (**S**), with just a few meters at the base in the gravelly soil (**G**), as shown in Fig. 6. The upper soil layers also have a significant inclination in the transversal direction (Fig. 6b).

The CNEL former library was investigated thoroughly too. The building is realized on a small hill (Fig. 7) overlooking Piazzale Flaminio and it is made of 6 storeys, the first three of which are partially underground on the north side. A plan view of the base level is reported in Figure 8. Endoscopic tests, flat-jack tests and sampling on the building identified a masonry bearing structure

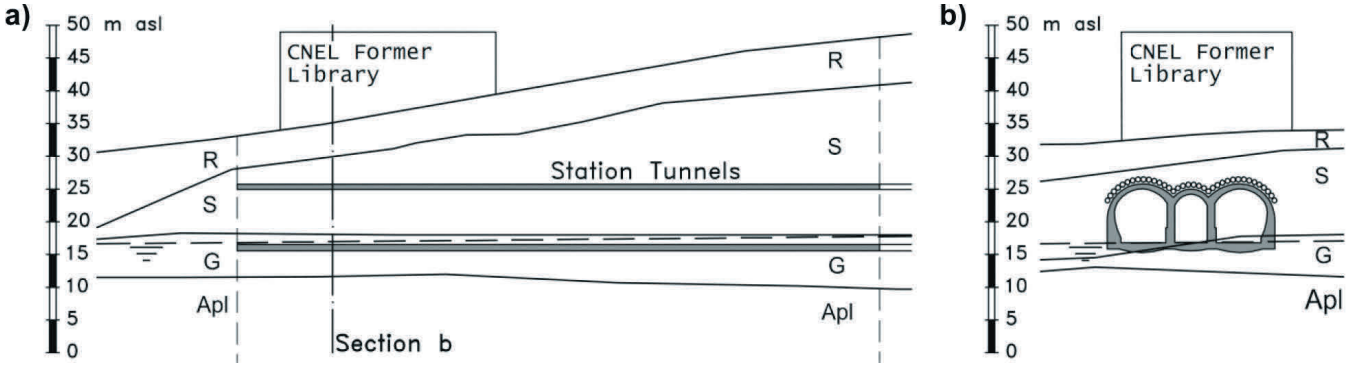

Figure 6. Geotechnical sections: a) longitudinal along the left tunnel; b) transversal at 15 m from the entrance.

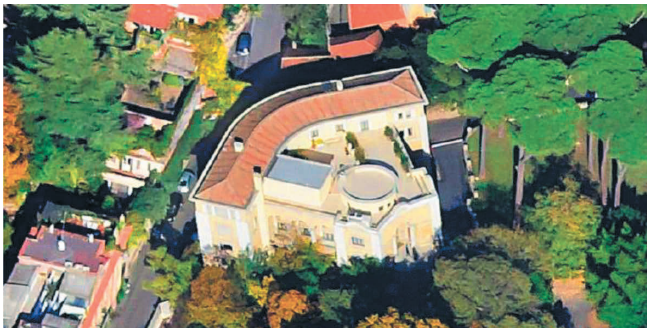

Figure 7. Aerial view of the CNEL former library.

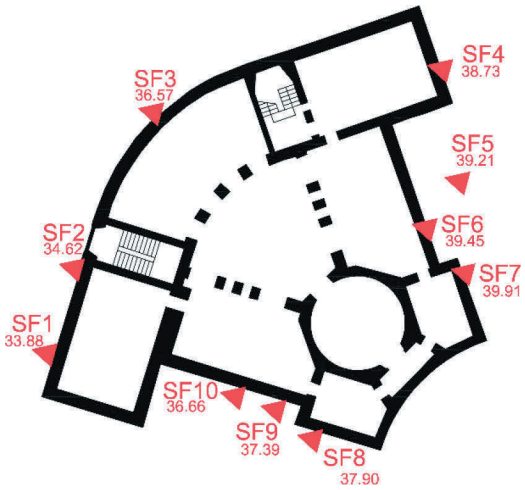

Figure 8. Plan view of the building's base level with location of the investigations of the foundation system.

with concrete and hollow tiles mixed floor slabs. The bearing walls are made both with natural elements and bricks.
The foundation system of the building was investigated directly through inclined continuous core sampling drillings and down-hole tests, that showed a continuous foundation made of bricks and stones randomly arranged, bonded with a weak cementation (i.e. rubble masonry). The foundations are based in the sandy soil (**S**) and therefore their elevation is quite variable and increases in the north direction following the natural inclination of the stratigraphy (see Fig. 6a).

4. Design solution

4.1. Technical and technological solutions

The excavation for the atrium, to be realized before the construction of the tunnels, is supported by perimetric pile walls. The piles are 27 m long, have a diameter *D* of 1 m and an inter-axis of 1.2 m on the north and east side (CNEL former library and Villa Borghese), while they are 27 m long, have a diameter of 1.5 m and inter-axis equal to1.7 m on the west side (towards Palazzo Alverà), as shown in Figure 9a. The pile walls are connected at the top with a reinforced concrete edge beam (2x1 m). The excavation has two levels of tubular steel struts (558.8 mm in diameter and thickness, *t*, of 9.52 mm) supporting the pile walls at the angles. The first level supports the top connecting edge beam and the second is located at a lower level (+27.5 m asl) where a second horizontal edge beam is realized (Fig. 9b). Finally, at the bottom, a reinforced concrete slab 1 m thick near the perimeter and 1.5 m thick in the central area, will be realized. Figure 10 shows the advancement of the excavation and the installation of the steel struts.
During the excavation, a stretch of the ancient consular road Fla-

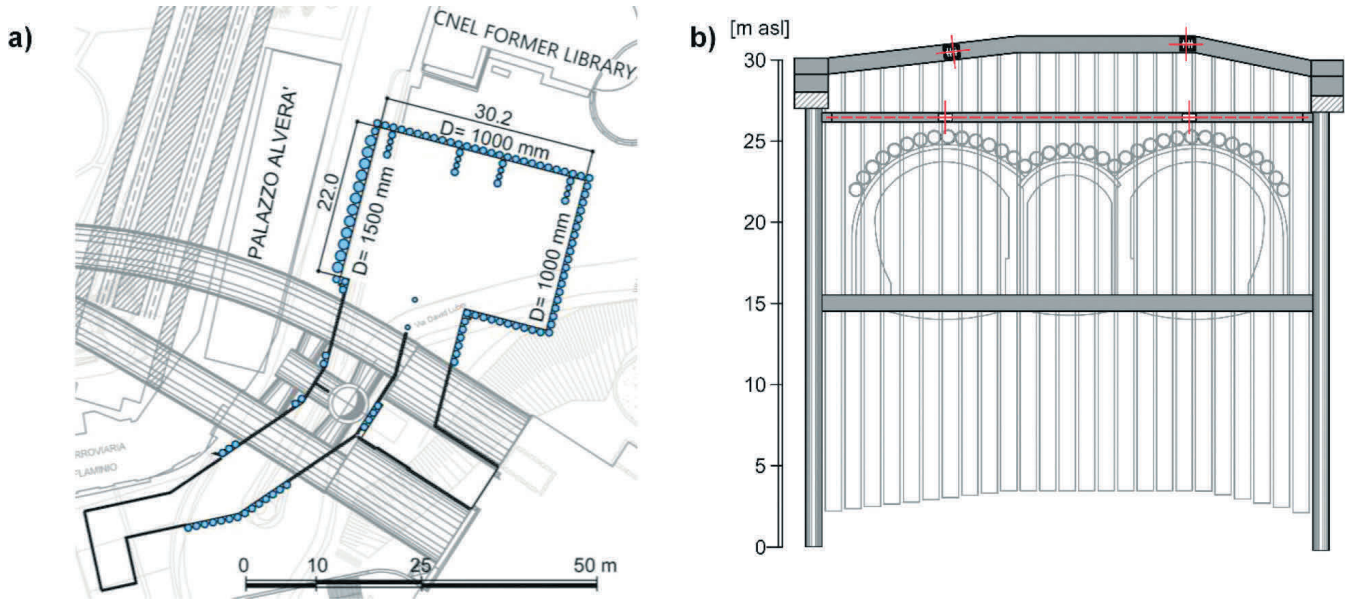

Figure 9. Atrium excavations: a) plan view of supporting pile-walls; b) north section (tunnel entrance).

Figure 10. Excavation of the atrium and installation of the steel struts.

Figure 11. Discover of a stretch of the ancient consular road Flaminia.

mina was discovered (Fig. 11). The archaeological finding was then disassembled and will be put back together on the surface upon completion of the works, enriching the beauty of Villa Borghese.
The excavation of the station tunnel will start from a reinforced concrete entrance portal, founded on 4 groups of 4 piles placed perpendicularly to the north wall. As previously anticipated, the three station tunnels will be around 100 m long and for the first stretch of 50 m, in average, will be slightly below, or even in touch, with the building's foundation. Furthermore, the station is almost as wide as the building (see Fig. 4), thus its construction involves the removal of the entire volume of foundation soils. Due to the significant volume of excavated soil and the challenging location of both the atrium and the station, especially with respect to the CNEL building, significant ground improvement works and protective measures were planned.
Below the building, the excavation section type A will be adopted (Fig. 12). The works involve the preliminary installation of 36 horizontal steel pipes (D = 813 mm, t = 12.5 mm), located just above the extrados of the tunnel and with a length dependent on the building's one (50 m in average). The steel pipes will be put in place using a MTBM, starting from the entrance pile wall. The MTBM has a retractile head and a system of jacks able to exert a thrust force of 2500 kN. The head is connected to the shield and the shield with the steel pipes. Once the excavation is completed, the final part of the shield is left in place and the MTBM retracts. Due to environmental reasons, in fact, it was not possible to construct an extraction shaft for the MTBM. The excavated soil is extracted using a screw conveyor. The use of a slurry shield in this case was not a viable option since there were high chances of losing the perforation fluid through small cavities, old wells and/or locally fractured foundations. Figure 13 shows the MTBM and close-up views of the head and rear, while Figure 14 shows a moment of the installation of the pipes and the collar placed at the entrance to confine the lubricant bentonite filling the gap between the pipe and the excavation profile.
After the installation of the steel pipes, the annular gap between excavation and pipe is grouted and the pipes filled with class C28/35 concrete. Near the entrance, the concrete is reinforced with steel bars that serve as structural connection with the reinforced concrete portal realized inside the new atrium (Fig. 15 and Fig. 16).
The steel pipes primarily serve a pre-support function and are not structurally connected with each other. Their protective effect in

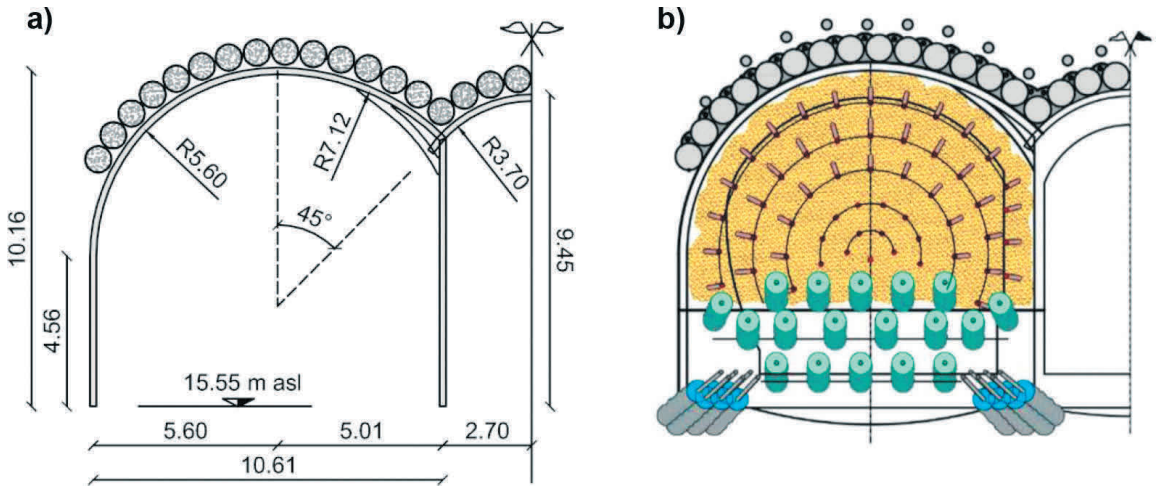

Figure 12. Excavation section type A: a) size; b) ground improvement at the face (from top to bottom: pre-support pipes, fiberglass elements and injections, jet grouting columns at the front and below the temporary lining).

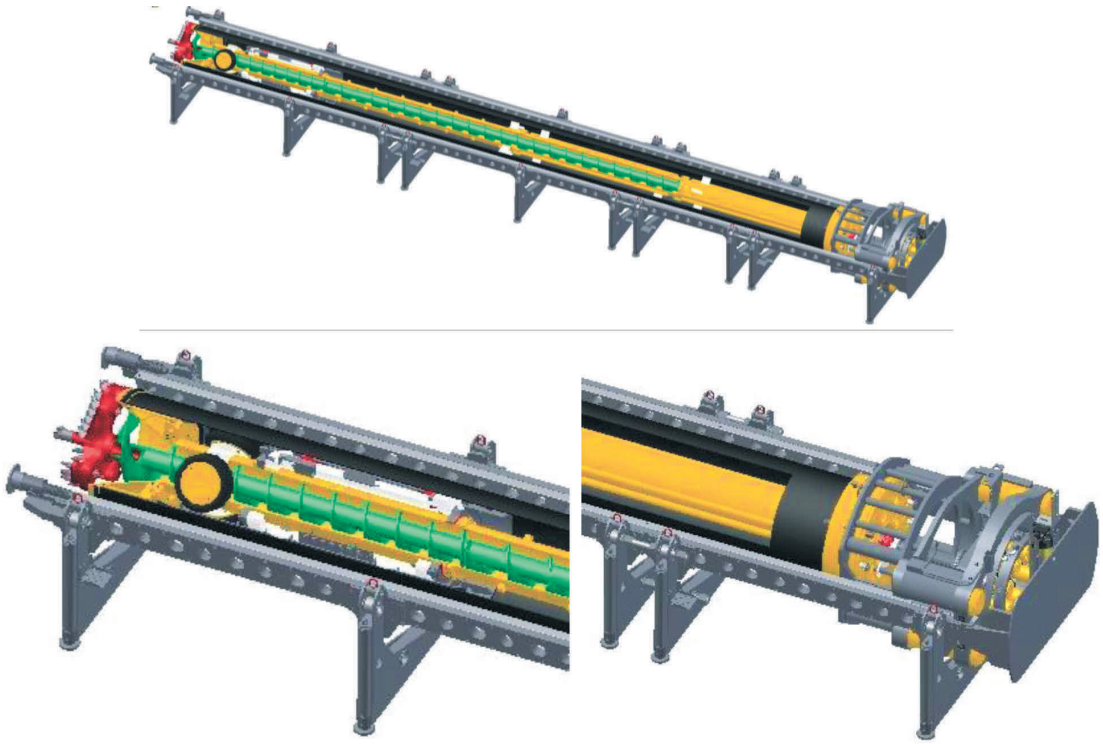

Figure 13. Micro Tunnel Boring Machine: global view and details.

the transversal direction, due to arch effect associated with the geometrical arrangement, is enhanced with an additional injection of a mixture of micro-cements, realized between the pipes for all their length. To this aim, 33 grout injection small pipes equipped with manchette valves spaced 50 cm will be employed.
The upper part of the excavation front, where the sands are, will be reinforced using fiberglass elements 16 m long. The fiberglass elements are also equipped with valves to allow the injection of a micro-cement mixture that will improve the surrounding soil. The lower part of the face, made of gravel, will be reinforced with jet-grouting columns 18 m long. Due to the presence of fines, the sandy gravel is not effectively injectable at low pressure. The reinforcements will be executed 8 m at a time. Additional jet-grouting columns, 12 m in length, will be realized to reinforce the gravelly soil at the base of the temporary lining. The ground improvement works are summarized in Fig. 17.

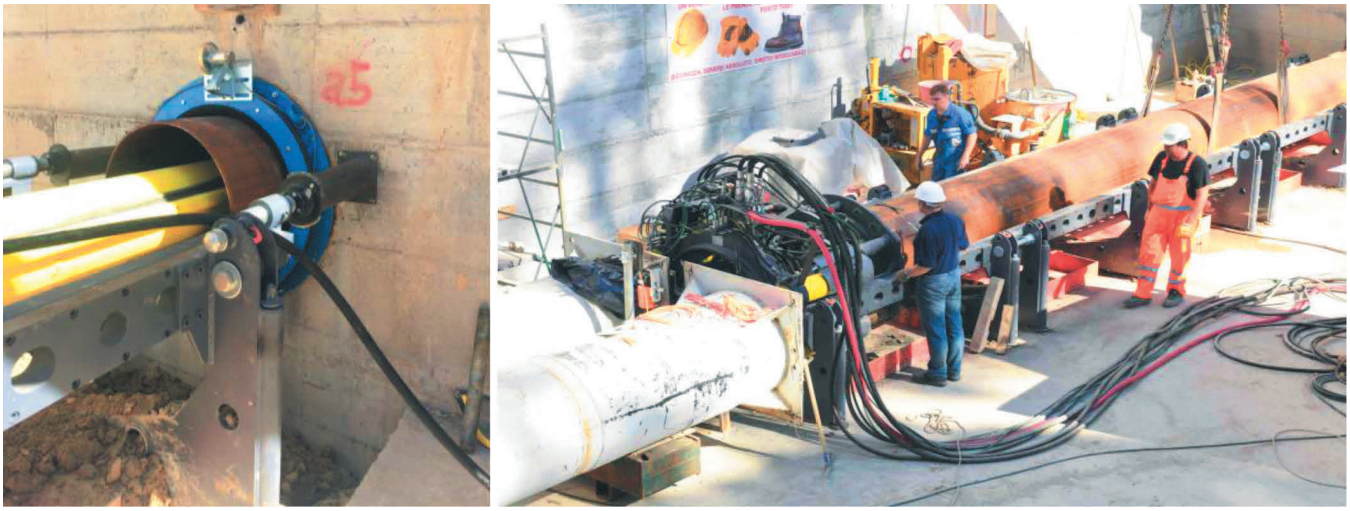

Figure 14. Installation of the steel pipes using the MTBM.

Figure 15. Steel pipes installed and steel bars in place for the connection with the entrance portal.

The temporary lining is made of steel ribs HEB200 with interaxis of 1 m and 25 cm of shotcrete (Fig. 18). The steel ribs have mechanical jacks at their base for loading immediately after the installation (active ribs). The final lining will be made of reinforced concrete, constructed 4 m at a time. In particular, the invert will be realized starting from a maximum distance of 4 m from the excavation front and will cover the entire space up to the face, while the upper part of the lining will be realized from a maximum distance of 8 m from the excavation face and will arrive at 4 m.

Overall, the designed excavation section is very heavily reinforced. As reported in the following paragraphs, this was necessary to minimize the settlement induced on the above building.
Once the excavation will surpass the CNEL building, the remaining part of the station tunnels will be constructed adopting a lighter excavation section (type B), characterized by the reinforcement of the roof with sub-horizontal concrete-injected steel pipes, 12 m long and overlapped by 4 m, for the left and right tunnels, and with fiberglass nails, 16 m long, for the central tunnel. The temporary lining will be the same of section type A, while the final lining will

Figure 16. Construction of the reinforced concrete entrance portal.

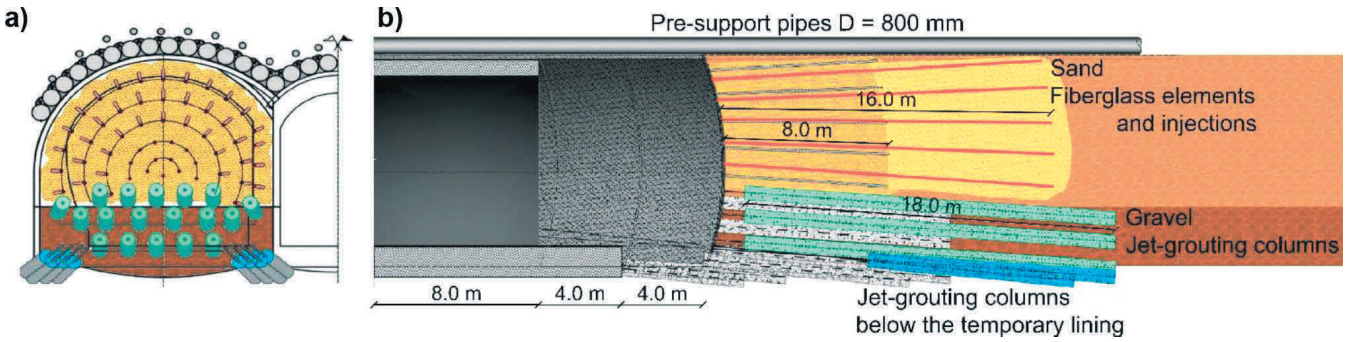

Figure 17. Ground improvements in the upper and lower part of the excavation face.

be put in place at a maximum distance from the excavation front of 16 m and 24 m, respectively for the invert and for the crown.
Summing up, the works sequence is the following:
1) construction of the pile-walls;
2) excavation down to +24 m asl and first level of microtunnelling;
3) completion of the microtunnelling with successive excavations down to +21.6 m asl;
4) construction of the entrance portal structurally connected with the steel pipes;
5) completion of the excavation down to +15.55 m asl and construction of the foundation slab;
6) excavation of the lateral tunnels: specifically, the front of the right one is maintained 24 m ahead of the left one;
7) excavation of the central tunnel.

Figure 18. Roof support system and lining elements.

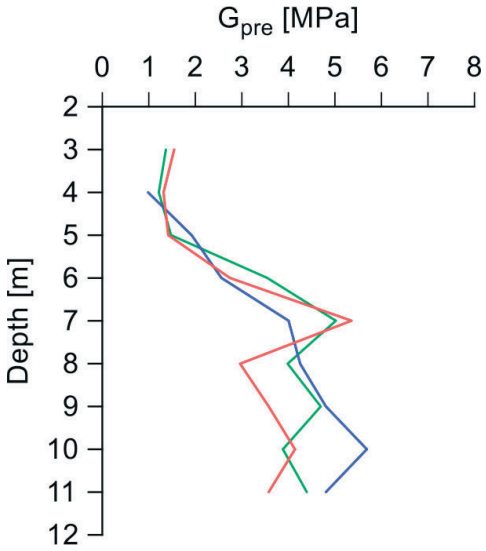

Figure 19. Pre-injections cross-hole tests results.

After the construction of the entrance portal (phase 4), in November 2017, the works stopped due to contractual problems and financial issues of ATAC. After a two-year hiatus, the works are going to recommence in January 2020 with the completion of the excavation of the atrium.

4.2. Field tests

The details of the ground improvement design were based on the results of a field test aimed at defining materials, technology and operational aspects; in particular, several kind of cement mixes, volumes and injection pressures were tested with the goal of quantifying the effectiveness of the treatment in terms of improvements in strength and stiffness of the sandy soil.

The field tests results allowed to identify the final solution, which consists of a micro-cement mixture. In particular, the ground improvement was designed as follows: i) injections near the pre-confinement pipes realized between the pipes using elements with valves every 50 cm, a maximum pressure of 3 MPa and a volume of 140 l/m; 2) pre-treatment of the front nucleus via 131 fiberglass elements having a diameter of 60/10 mm (55 elements for each lateral tunnel and 21 for the central one) injected with micro-cement via 50 cm spaced valves at a maximum pressure of 3 MPa for a volume of 200 l/m.

The field tests unexpectedly showed that the sandy gravel stratum is not injectable at low pressure. This feature was attributed to the very dense soil structure together with presence of fines.

The increment in stiffness was determined through cross-hole tests performed pre- and post-injections. The results showed an average increase of about 300% of the shear modulus *G* of the treated sand. Figure 19 reports the stiffness profiles determined before the injections, while Figure 20a reports the results of the test field in terms of ratio between post-injection and pre-injection shear moduli (G_{post}/G_{pre}) along three separate investigated profiles.

The increment in cohesion was investigated through laboratory tests, specifically uniaxial compression tests. Due to the heterogeneity of the samples retrieved in situ, the tests were carried out on specimens cemented in the laboratory. The specimens were prepared mixing crushed natural material (**S**, medium-fine silty sands) with the designed micro-cement mixture. The volume of cement mixture employed, V_{cem}, was able to fill the volume of the voids, V_v, in a percentage ranging between 30 to 100%. The value of effective cohesion, *c'*, obtained filling 50% of the voids with micro-cement – as expected in situ after the field tests – and assuming a constant value of friction angle of

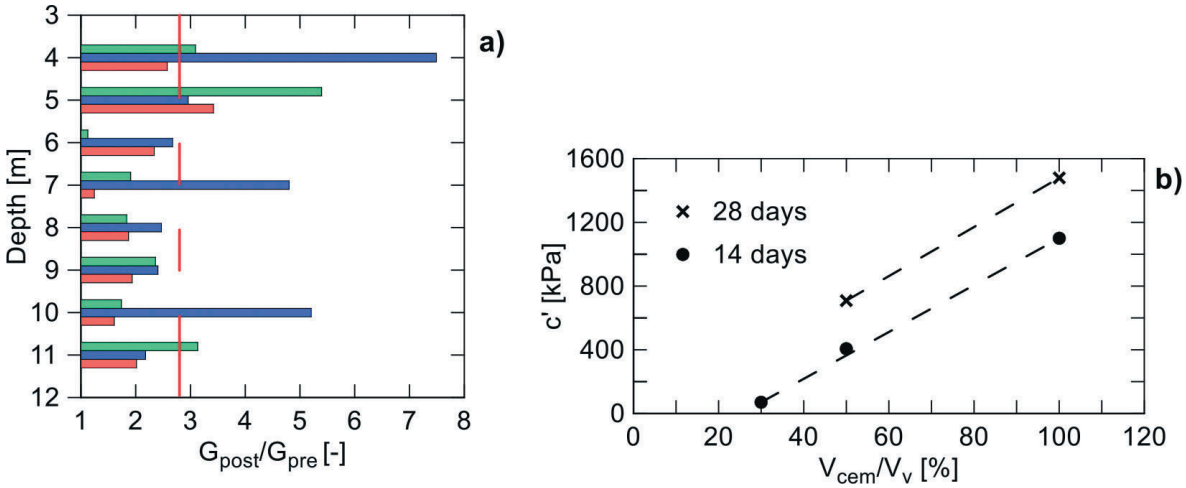

Figure 20. Field tests results: a) shear modulus; b) effective cohesion.

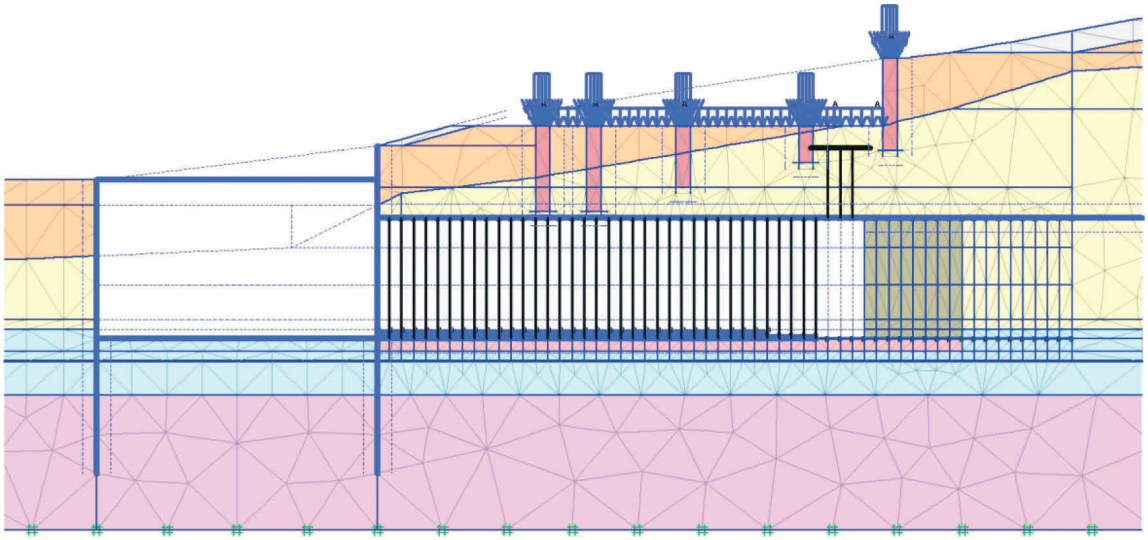

Figure 21. Longitudinal numerical model.

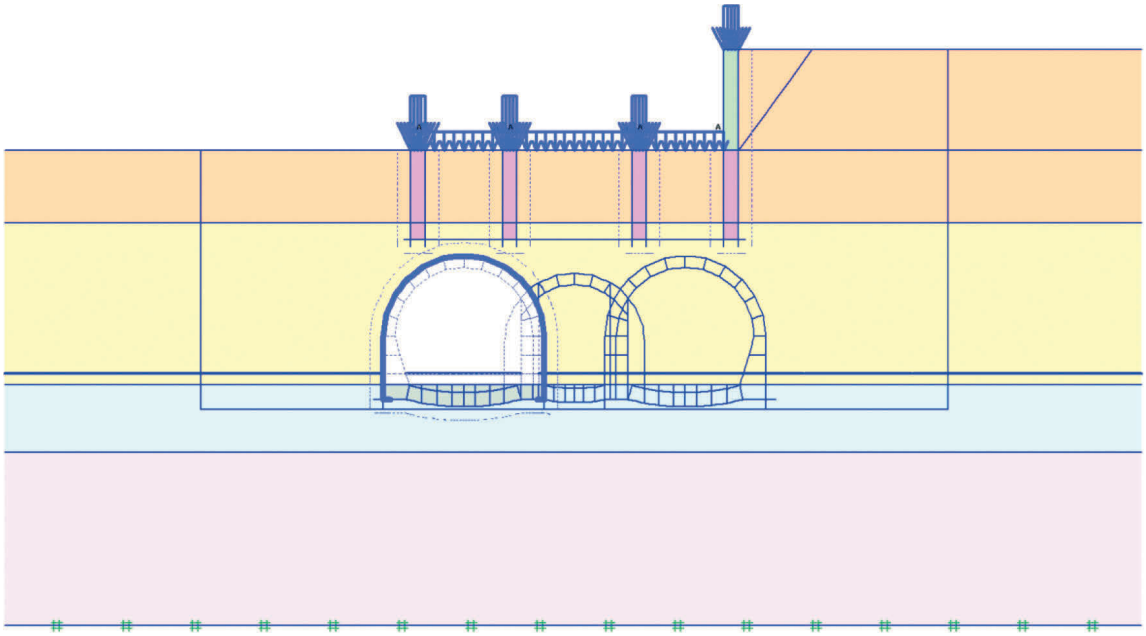

Figure 22. Transversal numerical model.

35° (equal to that of the natural untreated soil), after 28 days of curing, was 680 kPa, as illustrated in Fig. 20b, where the results are reported as a function of the percentage of filled voids. To account for the in-situ inhomogeneity of the treatments, a reduced value of c' = 150 kPa was assumed in the calculations.

4.3. Numerical analyses

As the computational times (both the time needed to set-up the model and actual runtime) associated with three-dimensional modelling are often not compatible with the variability of the choices naturally alternating during the engineering design process, the excavation was modelled two-dimensionally using the finite element commercial code Plaxis 2D. Being design analyses, the following constitute class A predictions (predictions made before the event), as defined by Lambe [38].

Two 2D numerical models were developed to analyse the excavation and refine the design choices: a longitudinal one (Fig. 21) and a transversal one (Fig. 22). The main purpose of the longitudinal analyses was the assessment of the effectiveness of the pre-support system and the definition of the ground improvement

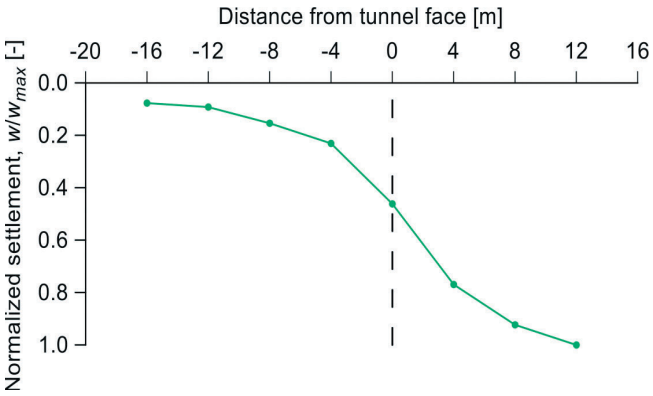

Figure 23. Longitudinal settlement profiles (the reference section is 20 m away from the entrance).

works, while the transversal analyses were used to evaluate the induced settlements.

In particular, a set of longitudinal parametric analyses was carried out to investigate several possible technical solutions, varying the length and the mechanical properties of the treated soil. The results of the longitudinal analyses were not used to evaluate the settlements - which are grossly overestimated as this model simulates an indefinite excavation in the out-of-plane horizontal direction - but just to analyse the efficacy of different design solutions. The chosen design solution was then implemented in a simplified (horizontal soil stratigraphy and simpler excavation phases) 3D model and, based on the observed pressure-displacement relations, the stress releases to be adopted in the cross-section analysis were defined.

The induced settlements were evaluated using the transversal model instead, which is clearly more suitable to simulate the behaviour of the entire system and allows to investigate the sequential excavations of the three tunnels.

For both models, the mesh size was chosen after a parametric study to ensure the lack of significant boundary effects influencing the numerical solution [39]. The boundaries' nodes on the right- and left-hand sides are fixed in the horizontal direction using rollers (only vertical displacements are allowed), the bottom boundary's nodes are fixed in all direction while those on the upper boundary are free to move.

The soil mechanical behaviour, as stated before, aiming at safe-side results, was simulated adopting a simple elastic perfectly plastic constitutive model with Mohr-Coulomb failure envelope employing the soil properties resulting from the geotechnical characterization and reported in Table 1 and zero dilatancy. Also, cautionary operative stiffness values associated to medium-large strains were adopted. The treated soil at the excavation front was simulated adopting the same constitutive model and assuming equivalent mechanical properties as determined through the field and laboratory tests showed in the previous paragraph (in the parametric longitudinal analyses these were varied). The transversal model takes indirectly into account the contribution of the flexural stiffness of the reinforcements on the longitudinal direction through the stress releases calculated in the longitudinal analyses.

Table 2. Main properties of the structural elements.

Unit	P (kN/m/m)	EA (kN/m)	EJ (kNm²/m)	ν (-)
MTBM	5.6	$2.295 \cdot 10^7$	$1.190 \cdot 10^6$	0.3
Pile wall (D = 1.0 m)	4.189	$2.346 \cdot 10^7$	$9.385 \cdot 10^5$	0.2
Steel struts	0.636	$1.668 \cdot 10^6$	$7.025 \cdot 10^4$	0.2
Bottom slab	15.0	$2.800 \cdot 10^7$	$2.333 \cdot 10^6$	0.2
Temporary lining*	7.1	$4.340 \cdot 10^6$	$3.106 \cdot 10^4$	0.2

* homogenised properties of the temporary lining adopted in the transversal analysis

The structural elements were modelled assuming an isotropic linear elastic behaviour; the properties of the main beam elements are listed in Table 2, where P is the unit weight, EA the axial stiffness and EJ the flexural stiffness. The pre-support pipes were modelled using beam elements in the longitudinal analysis and continuum elements with improved mechanical properties in the transversal one. In the longitudinal analyses the different support configurations (temporary lining, temporary lining and invert, final lining) were simulated using equivalent linear elastic springs, whose properties were calibrated performing further transversal analyses aimed at evaluating the lining behaviour under the expected pressure-displacement range. The foundation system of the CNEL former library was modelled via linear elastic continuum elements having E = 5 GPa and ν = 0.15. The superstructure was not modelled directly, but it was accounted for as an equivalent weight acting on the foundation, neglecting its stiffness.

The distribution of the pore pressure is governed by a piezometric surface located at +17 m asl. All the analyses were performed in

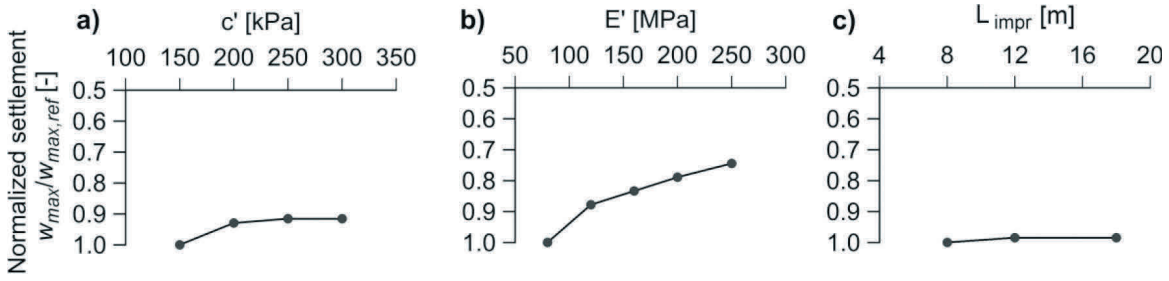

Figure 24. Parametric analyses: effects of the length and mechanical properties of the treated soil. The reference maximum settlement ($w_{max,ref}$) is obtained using respectively: a) c' = 150 kPa; b) E' = 80 MPa; c) L_{impr} = 8 m.

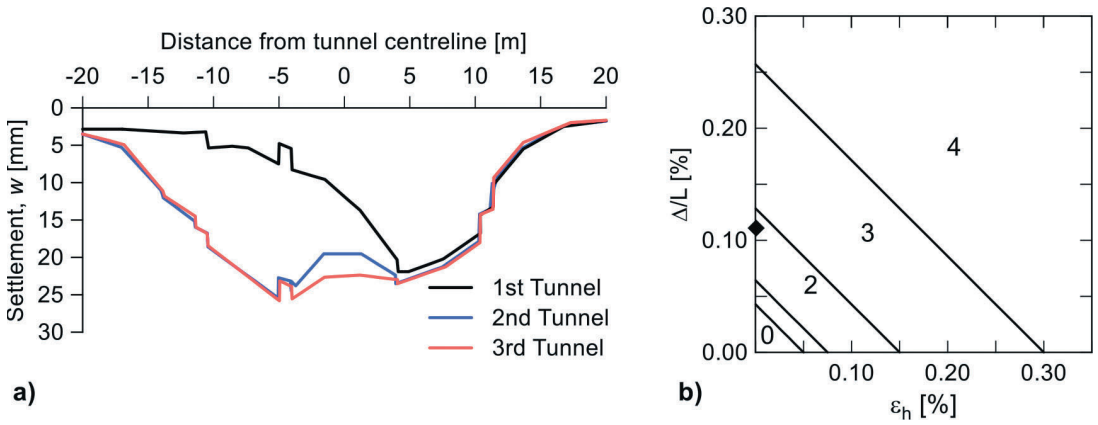

Figure 25. a) transversal vertical settlement profiles; b) evaluation of potential damage (damage category).

effective stress and, due to the high permeability of the soil close to the excavation, in drained conditions.

The results of the longitudinal analyses are reported in Fig. 23 in terms of normalized settlement, w/w_{max}, at the crown level in a section located at 20 m from the entrance portal. At the excavation face the settlement is about 50% of the final settlement. Figure 24 shows the results of the parametric study, performed varying the length and the mechanical properties of the treated soil. As it can be seen, values of cohesion of the treated area greater than 200 kPa do not have a significant influence (Fig. 24a). The same lack of beneficial effects was found for the lengths of superposition of the nucleus reinforcements (L_{impr}) for values greater that 8 m (Fig. 24c). On the other hand, the overall behaviour of the system was found to be more influence by the equivalent stiffness (E') of the treated soil (Fig. 24b).

The transversal analysis was used to obtain numerical predictions of the induced settlements and damages. The different phases of the excavations were simulated using different stress releases and according to the design work sequence. The following stress release factors, as obtained with the 3D simplified analyses, were adopted:

- unsupported excavation: stress release 10%;
- temporary lining: stress release 25%;
- temporary lining + final invert: stress release 50%;
- final lining: stress release 100%.

Figure 25a reports the transversal subsidence curves resulting the successive excavation of the three tunnels. The maximum settlement, located above the left tunnel, is roughly 25 mm. The settlements above the right tunnel are almost unaffected by the excavation of the left one (second excavated tunnel) and central one (last excavated). The horizontal displacements are close to zero.

The damage induced on the building was evaluated following the approach proposed by Burland (1995). The settlements and horizontal displacements at the surface, calculated considering the building-induced load and modelling the foundations but neglecting the stiffness of the building' superstructure, were used to determine the inflection ratios and identify the sagging and hogging areas. This approach allows to estimate the maximum expected elongation strains in the masonry and compare them with the damage categories proposed by the afore-mentioned Authors. As expected due to the small values of the horizontal displacements, the maximum value of horizontal strains, ε_h, at the foundation level was close to zero (Fig. 25b). The resulting expected damage induced by the excavation belongs to category 2, associated with slight functional damages.

5. 3D numerical modelling

After the design, a more advanced three-dimensional numerical model was developed using the finite element code Plaxis 3D v.2016 AE to investigate the influence of the simplified assumptions that have to be adopted when modelling in 2D the tunnelling-induced soil-structure interaction and to obtain more realistic and accurate results. In the case at hand, in fact, 3D modelling is especially helpful as it enables to simulate explicitly complex geometries (soils, structures and excavations) and articulated work sequences. As the tunnel excavation has yet to begin, these too constitute class A predictions.

5.1. The model

The numerical model, shown in Figure 26, has a transversal width of 120 m, a longitudinal length of 130 m and its centered on the tunnels. The base of the model is located about 3 diameters below the depth of the inverts to ensure the lack of boundary effects at the bottom. The nodes located on the vertical planes confining the model are restrained in the horizontal direction, while the nodes on the horizontal bottom plane are fixed in all directions. The elements of the mesh in the tunnels have a constant longitudinal length of 1 m, corresponding to the excavation steps simulated in the analyses. In order to improve the ability of the model of reproducing the behaviour of the entire system, the foundations and the structures of the first level of the building were simulated.

As done in the 2D design calculations, the analysis was carried out in drained conditions, assuming a hydrostatic pore pressure distribution governed by a piezometric level located at the base

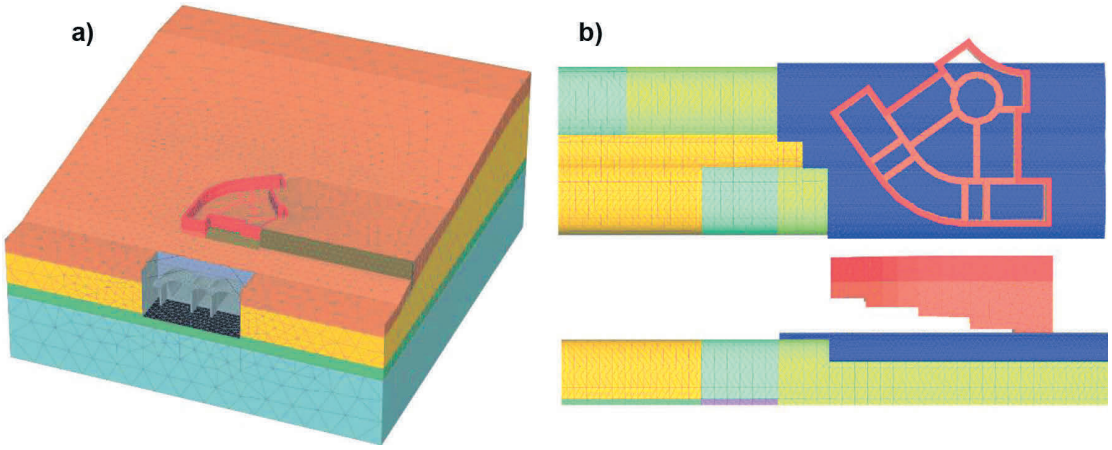

Figure 26. 3D numerical model: a) assonometric view; b) plan view and longitudinal section of the tunnels and foundations.

Table 3. Properties of the bi-dimensional plate elements.

Unit	P (kN/m/m)	EA (kN/m)	EJ (kNm²/m)
Pile wall (D = 1.0 m)	4.189	$2.346 \cdot 10^7$	$9.385 \cdot 10^5$
Pile wall (D = 1.5 m)	25.98	$33.87 \cdot 10^6$	$4.76 \cdot 10^6$
Raft foundations	25.00	$30.00 \cdot 10^6$	$2.25 \cdot 10^6$
Temporary lining	6.61	$41.40 \cdot 10^6$	$25.60 \cdot 10^6$

of the tunnels. Also, the same constitutive model, elastic perfectly plastic with Mohr-Coulomb strength criterion, and physical and mechanical soil properties (see Table 1) were adopted. The treated soil was modelled using the same constitutive model but with improved parameters according to the field tests results. The phases of the analysis are the following:

- equilibrium phase without the building;
- activation of the building elements and associated weight;
- excavation and activation of the atrium structures in several subphases, including those related to the activation of the pre-confinement pipes and the portal;
- progressive simulation of the excavation, supports installation and soil improvements.

The clayey and gravelly strata were modelled as horizontal, neglecting a slight inclination, while the sand and the man-made ground were modelled following the real stratigraphy resulting from the geotechnical investigations.

As per the building, the foundations and the perimetric walls of the underground stories were explicitly modelled, while the superstructure was taken into account just as an equivalent pressure. Differently from the design analyses, in this case the foundations were simulated adopting the real geometry, as reported in Figure 26b. Fig. 26b also shows, for a generic calculation phase, the areas where the soil was improved: the treatments at the face are shown in purple and cyan and the support pipes area in blue. The temporary lining is shown in green.

The foundation and the perimetric walls were modelled adopting an isotropic linear elastic constitutive model (E = 5 GPa, ν = 0.15). The pile walls, the foundation slab and the temporary lining were simulated using plate elements having a linear elastic behaviour (the adopted parameters are listed in Table 3). The temporary lining, made of shotcrete and steel ribs, was modelled as an equivalent homogenized section adopting the following parameters: $E_{shotcrete}$ = 10 GPa and E_{ribs} = 210 GPa. The 36 pre-confinement pipes were modelled according to their real length with just a slight geometrical simplification due to numerical reasons: since using cylindrical pipes would have required a higher number of mesh elements, the pipes' section was modelled as square and equivalent mechanical properties were given (the accuracy of the equivalence was preliminarily tested performing smaller-scale 3D analyses). The entrance portal was modelled in its entirety using continuum elements (linear elastic, E = 30 GPa) to reproduce the real level of restraint provided to the pipes. The final lining was modelled using continuum elements, respecting the real geometry of the lining, with a linear elastic behaviour and a Young's modulus of 30 GPa. The connecting edge beams were modelled using linear elastic beams elements (E = 30 GPa). Finally, the internal steel struts were simulated as elastic spring with a stiffness E = 210 GPa.

5.2. Numerical results

Figure 27 shows the settlements at the crown of the first and second tunnel respectively as a function of the distance from the excavation front in a section located at 20 m from the entrance pile wall (portal). The settlement at the face is 8 mm for the first tunnel and 10 mm for the second one; in both cases, the settlement at the front is about 40% of the final one. The gradient of the settlement curves is quite steep until the installation of the final lining, reaching about 65% of the final value.

The transversal settlements are reported in Figure 28 in a section located at 20 m from the entrance, which is the most critical due the relative position with respect to the building (Fig. 28a). The settlement profile at the level of the extrados of the supporting pipe-arch (+27 m asl) shows a final settlement trough almost

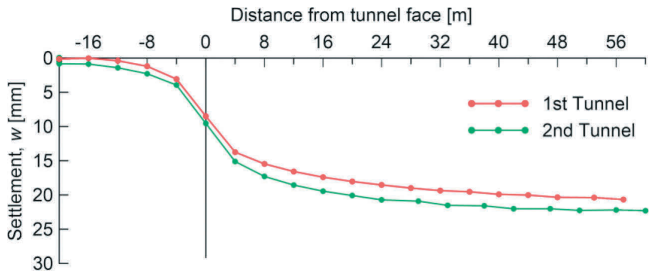

Figure 27. Longitudinal settlement profiles (the reference section is located 20 m away from the entrance portal).

symmetrical after the excavation of the three tunnels (Fig. 28b): compared to the design estimation, the maximum settlement above the left tunnel is similar to that above the right tunnel, showing that the deformations induced near the second tunnel by the excavation of the first one have a limited effect.
The settlement profiles at the surface (+35 m asl) are reported in Figure 28c. In particular, to illustrate the evolution of the settlements induced on the building, the figure shows the settlement profiles obtained at the design stage and those obtained with the 3D analysis at different advancements of the excavations. When the right excavation reaches a distance of 24 m - that is when the left excavation starts - the settlements due to the first tunnel have not achieved their maximum value yet; then, as the excavation proceeds, the settlements increase and the trough widens due to the excavation of the left tunnel, which reduces the distortions induced on the building. The final settlement trough is quite different than that obtained at the design stage; the maximum 3D settlement is about 30% less than its 2D counterpart.
Finally, Figure 29a shows the influence of the stiffness of the foundation system, which reduces the maximum settlements above both tunnels and thus limits the induced distortions. The symmetrical position of the building with respect to the final settlement trough due to the excavation three tunnels is associated with horizontal strains of elongation at its base. Adopting the same approach used at the design stage to evaluate the potential damage, the new inflection ratios cause a level of potential damage belonging to category 1, while the design analyses showed a level 2 damage (Fig. 29b).

6. Monitoring system

The installed pre-support pipes system and the heavily reinforced excavation section strongly reduce the risk of instability and potential damages. Furthermore, the expected value of induced settlements and damages is even smaller than predicted by the 3D analyses due to the cautionary choices of soil constitutive model and operative stiffness values. Nonetheless, due to the importance and vulnerability of the buildings in the area of the excavations, a particularly rich monitoring plan was designed.
The monitoring data will not be used to determine the excavation method and amount of reinforcements, as in an observational approach. The systematic control of the monitoring data and the

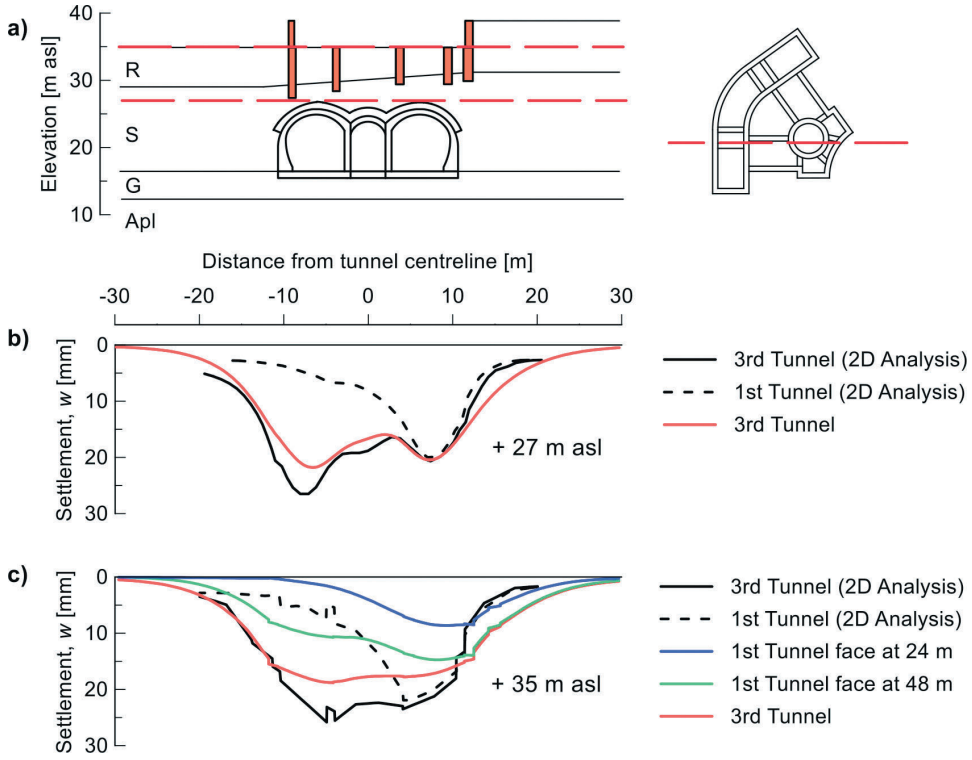

Figure 28. Transversal settlements profiles.

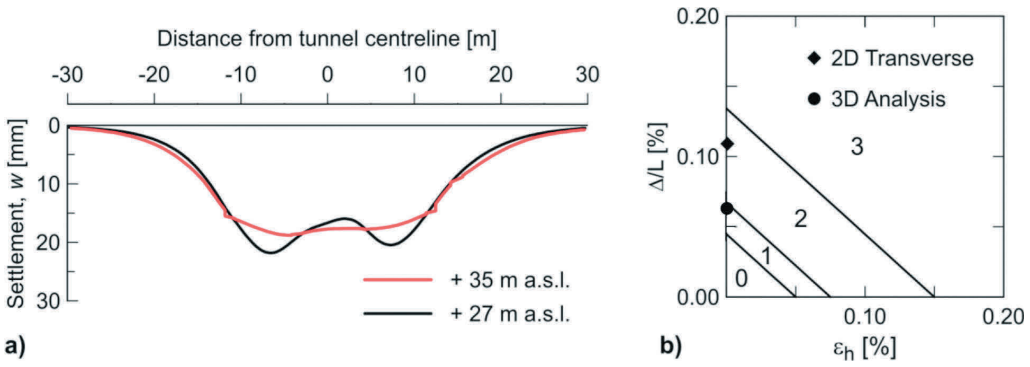

Figure 29. a) comparison between settlements profiles; b) evaluation of potential damage.

comparison with the developed calculation models will allow to confirm the settlements to be smaller than predicted and to evaluate the effects induced by the excavation on the surface, the behaviour of the geotechnical structures and the soil response. Also, the overall response showed by the monitoring system will allow to update the numerical models and re-calibrate them - particularly the operative stiffness value, which has a great influence on the response and it's practically impossible to define beforehand - based on the recorded behaviour, in order to improve the predictive capabilities while the excavation is still ongoing.

The settlements of the surface and of the buildings affected by the excavations of both the atrium and the tunnels (existing railway station, Palazzo Alverà, Villetta Ruffo, CNEL former library) will be monitored using 9 optical prisms and 47 topographic benchmarks for high-precision levelling. Moreover, the buildings are monitored internally with numerous displacements transducers (10÷30 per building) and tiltmeters (3 per building). The displacements of the pile-walls and internal struts will be recorded by 32 optical prisms, 3 inclinometers and 18 strain gauges installed on 6 struts (3 strain gauges each). In particular, 23 optical prisms will be installed on the top edge-beam, 4 on the secondary edge-beam (+27 m asl) and 5 on the entrance portal. The inclinometers will be installed inside 3 piles of the walls. The induced effects on the existing line A metro tunnel will be controlled through visual inspections, displacement transducers (in the eventuality of cracks opening) and strain gauges installed on the lining.

Finally, during the excavation of the station tunnels, each of the lateral tunnels temporary lining will be instrumented in 8 sections (five of which in the first 50 m of the tunnels, in the area most affected by the presence of the building) with:

– 5 optical prisms for the measurement of the convergences;
– 2 load cells;
– 3 couples of strain gauges;

Additionally, in each tunnel, two of the pipes constituting the pre-support will be monitored using removable horizontal inclinometers and once every two instrumented sections a geomechanical survey of the excavation face will be realized. The location of the monitoring instruments, most of which is already installed, is reported in Figure 30.

During the micro-tunnelling, the installation of the steel pipes and the concrete-filling, the response of the CNEL former library was kept under surveillance via high-precision levelling. The data showed an average settlement of about 3 mm, quite uniform throughout the benchmarks affected by the installation. Being the

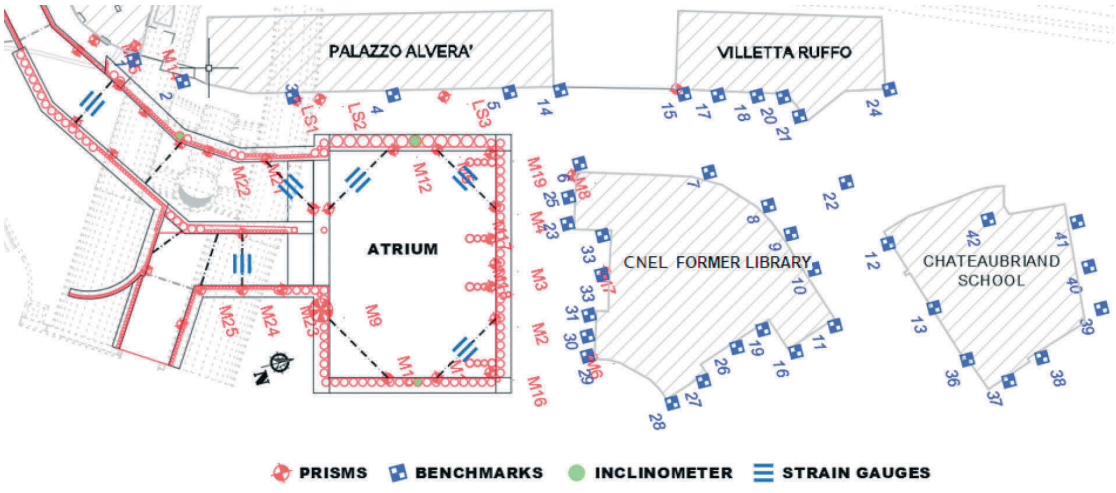

Figure 30. Monitoring plan.

settlements small in absolute values and the distortions close to zero, no appreciable effects were observed on the building.

7. Conclusions and future developments

Tunnelling in urban environment often presents significant technical and technological challenges, as in the case of the new underground railway station of Piazzale Flaminio in Rome, closely interacting with a historic masonry building, the CNEL former library. The paper presented the design solutions devised to minimize the risks associated to the conventional excavation of a three-tunnel station, including significant ground improvement works at the tunnel front and the installation of a stiff pre-support system prior to the start of the tunnel excavation. The pre-support system is composed of 36 horizontal steel pipes that were installed above the tunnels using a specially designed Micro Tunnel Boring Machines. The pipes were then filled with concrete and structurally connected at the entrance to a robust reinforced concrete portal founded on large piles. The works stopped in November 2017 when the atrium was partially excavated, immediately after the construction of the entrance portal, due to financial problems of the local authority in charge of the execution of the project. Until then, the works advanced regularly and very small displacements were recorded, with zero effects induced on the surrounding buildings.
At the design stage, a series of numerical analyses was performed using 2D models simulating the excavation both in the longitudinal and transversal planes; the former was developed to carry out parametric analyses aimed at identifying the relative influence of the ground improvement works and refine the design solution, the latter to evaluate the tunnelling-induced settlements. The results showed the effects of the sequential excavation of the three tunnels and allowed to estimate the potential induced damage, belonging to category 2 as defined by Burland.
After the design phase, a more advanced simulation was performed developing a 3D numerical model, able to simulate more accurately the real geometries, the phases of the excavation and the tunnel-soil-existing building interactions; the same soil properties were used. The results showed that the settlements, distortions and potential induced damage on the building (category 1) were smaller than predicted at the design stage.
The following main concluding remarks can be drawn:

- the injection field test allowed to define the micro-cement mixture and the injection volumes and pressures to be adopted. More importantly, it allowed to quantitatively determine the stiffening and strengthening effects of the treatment;
- the micro-tunnelling and the installation of the pipes induced very small surface settlements, confirming the effectiveness of the technical and technological solution adopted. The settlements measured by the benchmarks affected by the excavation were quite uniform and provided average values of just 3 mm;
- as expected, the results obtained at the design stage employing simplified 2D models provided safe-side results that, still, proved to be not too far off. Also, the simplified models enable to define and refine the technical design solutions through parametric analyses;
- the correct simulation of the real geometries and work phases plays a key role in this class of interaction problems, as highlighted by the three-dimensional analyses that showed that the design analyses overestimated the damage induced on the building.

In this study, a simple elastic perfectly plastic constitutive model with Mohr-Coulomb strength criterion was adopted and the values of the stiffness moduli used in the design calculations correspond to medium-large strain levels. Surely, a more accurate simulation of the soil mechanical behaviour, able to take into account the influence of the non-linearities of the soil response, would provide more realistic results, but that goes beyond the scope of this paper and will be the subject of future developments.
At the time of writing (December 2019), the works are soon to recommence after a two-years hiatus and will be completed in another couple of years. The next steps will be the completion of the excavation of the atrium and, finally, the excavation of the three-tunnel station. The rich monitoring system already put in place will allow to record a significant amount of data, providing the opportunity to evaluate the real behaviour of such a complex soil-structures interaction. The comparison between class A predictions, further numerical analyses performed using more advanced constitutive soil models and experimental results will allow to improve our knowledge of the specific behaviour of the special pre-support system installed and of the entire soil-tunnel-building system.

Acknowledgements

The Authors would like to acknowledge the contribution of GP Ingegneria Srl, particularly engineers G. Guiducci and E. Moscatelli, to the development of the project, engineers A. Zechini and D. Indelicato, who contributed to the design with their invaluable experience, and Pato Srl that helped designing the pipes' installation system and executed the installation.

References

[1] LUNARDI P., FOCARACCI, A., MERLO, S. (1997) – Mechanical pre-cutting for the construction of the 21.5 m span arch of the "Baldo degli Ubaldi" station. Gallerie e Grandi Opere Sotterranee, 53, 54-67.

[2] LUNARDI P. (1989) – A new large span tunnel construction method in non-cohesive soil: the "cellular arch". Gallerie e Grandi Opere Sotterranee, 29 (in Italian).

[3] PECK R. B. (1969). Deep excavations and tunneling in soft ground. Proc. 7th ICSMFE, 1969, 225-290.

[4] MOH Z.C., JU D.H., HWANG R.N. (1996) – Ground movements around tunnels in soft ground. In Proceedings International Symposium on Geotechnical Aspects of Underground Construction in Soft Ground (Vol. 730, pp. 725-730). London: Balkema AA.

[5] BURLAND J.B., WROTH C.P. (1974) – Settlement of buildings and associated damage. In Proceedings of Conference on Settlement of Structures. Pentech Press, Cambridge, pp. 611-654.

[6] BOSCARDIN M.D., CORDING E.J. (1989) – Building response to excavation-induced settlement. Journal of Geotechnical Engineering, 115 (1), 1-21.

[7] Burland J.B. (1995) – Assessment of risk of damage to building due to tunnelling and excavation. In Proceedings of the 1 st International Conference on Earthquake Geotechnical Engineering, pp. 1189-1201.

[8] Miliziano S., Soccodato F.M., Burghignoli A. (2002) – Evaluation of damage in masonry buildings due to tunnelling in clayey soils. In Proceedings of the 3rd International Symposium on Geotechnical Aspects of Underground Construction in Soft Ground, Toulouse, 2002. Balkema, Rotterdam, pp. 335-340.

[9] Tamagnini C., Miriano C., Sellari E., Cipollone N. (2005) – Two-dimensional FE analysis of ground movements induced by shield tunnelling: the role of tunnel ovalization. Rivista Italiana di Geotecnica 1, 11-33.

[10] Altamura G., Burghignoli A., Miliziano S. (2007) – Modelling of surface settlements induced by tunnel excavation using the differential stress release technique. Rivista Italiana di Geotecnica 41 (3), 33-47.

[11] Möller S.C., Vermeer P.A. (2008) – On numerical simulation of tunnel installation. Tunnelling and Underground Space Technology, 23 (4), 461-475.

[12] Galli G., Grimaldi A., Leonardi A. (2004) – Three-dimensional modelling of tunnel excavation and lining. Computers and Geotechnics, 31 (3), 171-183.

[13] Svoboda T., Masin D. (2011) – Comparison of displacement field predicted by 2D and 3D finite element modelling of shallow NATM tunnels in clays. Geotechnik, 34(2), 115-126.

[14] Janin J. P., Dias D.F.R.H., Emeriault F., Kastner R., Le Bissonnais H., Guilloux A. (2015) – Numerical back-analysis of the southern Toulon tunnel measurements: A comparison of 3D and 2D approaches. Engineering geology, 195, 42-52.

[15] Kasper T., Meschke G. (2004) – A 3D finite element simulation model for TBM tunnelling in soft ground. International Journal of Numerical Analytical Methods in Geomechanics, 28 (14), 1441-1460.

[16] Kavvadas M., Litsas D., Vazaios I., Fortsakis P. (2017) – Development of a 3D finite element model for shield EPB tunnelling. Tunnelling and Underground Space Technology, 65, 22-34.

[17] de Lillis A., De Gori V., Miliziano S. (2018) – Numerical modelling strategy to accurately assess lining stresses in mechanized tunneling. In Numerical Methods in Geotechnical Engineering IX, Volume 2 (pp. 1295-1302). CRC Press.

[18] De Gori V., De Lillis A., Miliziano S. (2019) – Lining stresses in a TBM-driven tunnel: A comparison between numerical results and monitoring data. In Tunnels and Underground Cities. Engineering and Innovation Meet Archaeology, Architecture and Art (pp. 3634-3643). CRC Press.

[19] Callari C., Casini S. (2005) – Tunnels in saturated elasto-plastic soils: three-dimensional validation of a plane simulation procedure, Mechanical Modelling and Computational Issues in Civil Engineering, M. Frémond & F. Maceri (Eds.), Springer, 2005, 143-164.

[20] Callari C., Casini S. (2006) – Three-dimensional analysis of shallow tunnels in saturated soft ground, Geotechnical Aspects of Underground Construction in Soft Ground - Fifth Int. Symp. TC28, 2006, Balkema, 495-501.

[21] Maleki M., Sereshteh H., Mousivand M., Bayat M. (2011) – An equivalent beam model for the analysis of tunnel-building interaction. Tunnelling and Underground Space Technology, 26 (4), 524-533.

[22] Farrell R., Mair R., Sciotti A., Pigorini A. (2014) – Building response to tunnelling. Soils and Foundation, 54 (3), 269-279.

[23] Losacco N., Burghignoli A., Callisto L. (2014) – Uncoupled evaluation of the structural damage induced by tunnelling. Géotechnique, 64 (8), 646-656.

[24] Bilotta E., Paolillo A., Russo G., Aversa S. (2017) – Displacements induced by tunnelling under a historical building. Tunnelling and Underground Space Technology, 61, 221-232.

[25] Giardina G., Hendriks M.A.N., Rots J.G. (2015) – Sensitivity study on tunnelling induced damage to a masonry façade. Engineering Structures, 89, 111-129.

[26] Fargnoli V., Boldini D., Amorosi A. (2015) – Twin tunnel excavation in coarse grained soils: observations and numerical back-predictions under free field conditions and in presence of a surface structure. Tunnelling and Underground Space Technology, 49, 454-469.

[27] Franza A., Marshall A.M., Haji T., Abdelatif A.O., Carbonari S., Morici M. (2017) – A simplified elastic analysis of tunnel-piled structure interaction. Tunnelling and Underground Space Technology, 61, 104-121.

[28] Miliziano S., de Lillis A. (2019) – Predicted and observed settlements induced by the mechanized tunnel excavation of metro line C near S. Giovanni station in Rome. Tunnelling and Underground Space Technology, 86, 236-246.

[29] Ventriglia U. (2002) – Geology of the City of Rome, Amministrazione Provinciale di Roma, Roma (in Italian).

[30] Schmertmann J.H. (1978) – Guidelines for cone penetration test performance and design. Report n 78-209, U.S. Department of transportation, Federal Highway Administration, Washington, D.C.

[31] Denver H – (1982) – Modulus of elasticity for sand determined by SPT and CPT. In Proceedings of the 2nd European Symposium on Penetration Testing, Amsterdam, pp. 24-27.

[32] Mènard L. (1976) – Règles Relatives à l'Exécution des Essais Pressiométriques. Sols Soils 7 (27)

[33] Mair R.J., Wood D.M. (1987) – Pressure meter testing: methods and interpretation. CIRIA Ground Engineering Report, Butterworths, London.

[34] Rotisciani G.M., Miliziano S. (2014) – Guidelines for calibration and use of the Severn-Trent sand model in modeling cantilevered wall-supported excavations. International Journal of Geomechanics, 14 (6), 04014029.

[35] Rotisciani G.M., Miliziano S., Sacconi S. (2015) – Design, construction and monitoring of a building with deep basements in Rome. Canadian Geotechnical Journal, 53 (2), 210-224.

[36] NTC (2008). Norme Tecniche per le Costruzioni, DM 14/01/2008, GU n.29 del 04/02/2008, Suppl. Ord. 30 (in Italian).

[37] Mayne P.W., Kulhawy F.H. (1982) – K0-OCR relationships in soil. Journal of Soil Mechnics and Foundation Division, 108 (6), 851-872.

[38] Lambe T.W. (1973) – Predictions in soil engineering. Géotechnique, 23(2), 151-202.

[39] Franzius J.N., Potts D.M. (2005) – Influence of mesh geometry on three-dimensional finite element analysis of tunnel excavation. International Journal of Geomechanics, 5 (3), 256-266.